Inorg. Chem. **2008**, *47*, 1874−1876

Inorganic Chemistry
Communication

On the 2-Electron 3-Center B−H−B Bond: Charge Density Determination of Tetraborane(10)

Diana Förster,[†] Christian B. Hübschle,[†] Peter Luger,[†] Thomas Hügle,[‡] and Dieter Lentz*[,‡]

Institut für Chemie und Biochemie/Anorganische Chemie, Freie Universität Berlin, Fabeckstrasse 34−36, 14195 Berlin, Germany, and Institut für Chemie und Biochemie/Kristallographie, Freie Universität Berlin, Fabeckstrasse 36a, 14195 Berlin, Germany

Received September 28, 2007

In order to characterize the 2-electron 3-center hydride bridges in *arachno*-tetraborane, an experimental charge-density study was performed complemented with various theoretical calculations. The charge-density distribution and its topological properties were analyzed according to the "atoms in molecules" theory of Bader. The asymmetric bonding situation of the highly polarized hydride bridges is discussed in detail.

Boranes[1] form a fascinating class of chemical compounds. The structures of β-diborane(6),[2] tetraborane(10),[3] pentaborane(9),[4] and pentaborane(11)[5] were elucidated by X-ray diffraction analysis in the pioneering work of Lipscomb et al. in the 1950s. Because of their very interesting bonding situations caused by the occurrence of 2-electron multicenter bonds, boranes are still a field of research. Since the early theoretical work of Longuet-Higgins and Bell, numerous theoretical contributions[6] on the structure and bonding of boranes and carboranes have been published including a topological analysis of the charge density from theoretical data by Bader et al.[7]

Experimental charge-density determinations on boron hydrogen compounds were carried out for β-diborane(6),[8] decaborane(14),[9] four carboranes,[10−12] and recently the *closo*-$B_6H_7^-$, in which one boron triangle is capped by a H atom.[13] Herein, we report the charge-density analysis of tetraborane(10) based on high-resolution X-ray data (sin $\theta/\lambda_{max} = 1.11$ Å^{-1})[14] and additional theoretical calculations.[22]

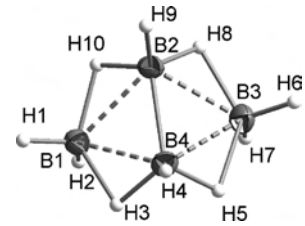

Figure 1. Structure and labeling scheme of B_4H_{10}.[16]

According to the Wade rules,[15] tetraborane(10) (Figure 1) forms an arachno structure with 14 skeletal electrons by removing two neighboring vertexes from an octahedral cage.

The topological analysis[18] of the charge density was carried out using the formalism of the theory of "atoms in

* To whom correspondence should be addressed. E-mail: lentz@chemie.fu-berlin.de.
† Institut für Chemie und Biochemie/Kristallographie.
‡ Institut für Chemie und Biochemie/Anorganische Chemie.

(1) *Boron Hydride Chemistry*; Muetterties, E. L., Ed.; Academic Press: New York, 1975. Wiberg, E.; Amberger, E. *Hydrides of the Elements of Main Groups O-IV*; Elsevier: Amsterdam, The Netherlands, 1971. Lipscomb, W. N. *Boron Hydrides*; W. A. Benjamin: New York, 1963.
(2) Smith, H. W.; Lipscomb, W. N. *J. Chem. Phys.* **1965**, *43*, 1060–1064.
(3) Nordman, C. E.; Lipscomb, W. N. *J. Chem. Phys.* **1953**, *23*, 1856–1864.
(4) (a) Dulmage, W. J.; Lipscomb, W. N. *Acta Crystallogr.* **1952**, *5*, 260–264. (b) Nordman, C. E. *J. Mol. Struct.* **1999**, *485–486*, 299–203.
(5) Lavine, L. R.; Lipscomb, W. N. *J. Chem. Phys.* **1954**, *22*, 614–620.
(6) (a) Longuet-Higgins, H. C.; Bell, R. P. *J. Chem. Soc.* **1943**, 250. (b) Xi Tian, S. *J. Phys. Chem.* **2005**, *A 109*, 5471–5480. (c) Böyükata, M.; Özdogan, C.; Günvenc, Z. B. *THEOCHEM* **2007**, *805*, 91–100.
(7) Bader, R. F. W.; Legare, D. A. *Can. J. Chem.* **1992**, *70*, 657–676.
(8) Hübschle, C. B.; Messerschmidt, M.; Lentz, D.; Luger, P. *Z. Anorg. Allg. Chem.* **2004**, *630*, 1313–1316.
(9) (a) Dietrich, H.; Scheringer, C. *Acta Crystallogr.* **1978**, *B34*, 54–63. (b) Brill, R.; Dietrich, H.; Dierks, H. *Acta Crystallogr.* **1971**, *B27*, 2003–2018.
(10) Antipin, M.; Boese, R.; Bläser, D.; Maulitz, A. *J. Am. Chem. Soc.* **1997**, *119*, 326–333.
(11) Lysenko, K. A.; Antipin, M.; Yu, M.; Lebedev, V. N. *Inorg. Chem.* **1998**, *37*, 5834–5843.
(12) Glukhov, I. V.; Lyssenko, K. A.; Korlyuokov, A. A.; Antipin, M. Y. *Faraday Discuss.* **2007**, 203–215. Glukhov, I. V.; Lyssenko, K. A.; Antipin, M. Y. *Struct. Chem.* **2007**, *18*, 465–469.
(13) Förster, D.; Scheins, S.; Luger, P.; Lentz, D.; Preetz, W. *Eur. J. Inorg. Chem.* **2007**, *20*, 3169–3171. Hofmann, K.; Prosenc, M. H.; Albert, B. R. *Chem. Commun.* **2007**, 3097–3099.
(14) Crystal data: monoclinic, $P2_1/n$, $a = 5.789(2)$ Å, $b = 10.135(3)$ Å, $c = 8.690(2)$ Å, $\beta = 106.037(6)°$, $V = 490.0(2)$ Å^3, $Z = 4$, $\rho = 0.723(3)$ g cm^{-3}, $T = 98(2)$ K, λ(Mo Kα) = 0.710 73 Å, $2\theta_{max} = 104.61°$; 26 256 reflections measured, 5320 crystallographically independent ($R_{int} = 0.050$); 3251 observed ($>3\sigma$); completeness 94.6%; redundancy 4.5. The structure was solved by direct methods and refined using full-matrix least-squares methods (*SHELX97*).[29] Multipole refinement using *XD*;[19,20] 101 parameters, B atoms, anisotropic displacement parameters, multipole refinement up to hexadecapolar level, H atoms: isotropic, B−H distances fixed to theoretical values[17] (B−H term = 1.18 Å; B−H$_{bridge}$ = 1.26/1.42 Å), multipole refinement up to the quadrupolar level; multipole parameters constraint to C_{2v} symmetry of the molecule; $R_1 = 0.031$; $R_{all} = 0.054$; GOF = 1.13; residual density (min/max/rms): −0.226/0.126/0.032 e/Å^3.
(15) (a) Wade, K. *Chem. Commun.* **1971**, 792–793. (b) Wade, K. *Adv. Inorg. Radiochem.* **1976**, *18*, 1–67.

10.1021/ic701924r CCC: $40.75
Published on Web 02/14/2008

molecules" (AIM) developed by Bader,[21] which was complemented with some theoretical calculations.[22] Although there exists some controversy about the limits of the AIM model,[24,25] the analysis of the values of the electron density (Table 1) ρ_{BCP} and the Laplacians $\nabla^2\rho_{BCP}$ at the bond critical points (BCPs) has the advantage of enabling a quantitative description of bonds from charge-density distributions obtained experimentally and/or theoretically.

The charge-density values on the BCPs of all B−H_{term} bonds are very similar, and the Laplacian values are negative as they are for the B2−B4 bond, indicating covalent bonds. Furthermore, BCPs are detected on the μ-bridging B−H_{bridge} bond paths, while there are no BCPs on the bridged B−B connection lines B1−B2, B2−B3, B3−B4, and B4−B1, respectively. This phenomenon could be found earlier in the charge-density analysis of diborane(6)[8] and $B_6H_7^-$.[13]

Consequently, one ring critical point is found for each of the five-membered rings formed by B2,B4,H5,B3,H8 and B2,B4,H3, B1,H10, respectively. In general, the interactions among three atoms are associated with a variety of molecular graphs.[21] However, this is not necessarily associated with three separated and localized bonds forming a three-membered ring. Inward curvature of the bond paths is often an indication for a delocalized bond, whereas outward curvature of the paths is typical of three localized bonds.[26] Figure 2 (left) exhibits the bond paths of tetraborane. As can be seen, all bond paths included in 2-electron 3-center (2e-3c) bonds are curved inward. The B−H_{term} bonds are 2e-2c bonds and therefore straight. Consequently, the bond paths of the long B−H_{bridge} are significantly longer (by 0.06 Å from experiment and even more than 0.1 Å from theory; Table 1) than the direct interatomic distances, whereas no difference between the direct distance and path length exists for B−H_{term} bonds. The B2−B4 bond shows concave curvature, which can be explained by the repulsive effect of the terminal H atoms.

Table 1. Bond Topological Properties of B_4H_{10}[a]

bond	method	distance	path	ρ_{BCP} (e/Å^3)	$\nabla^2\rho_{BCP}$ (e/Å^5)
B2−B4	exp	1.7251(4)	1.730	0.87(1)	−2.9(1)
	B3/exp	1.7251	1.728	0.90	−5.3
	B3/opt	1.7206	1.724	0.91	−5.4
	HF/opt	1.7445	1.750	0.92	−6.4
	MP2/opt	1.7295	1.777	0.94	−6.5
	B3+/opt	1.7165	1.720	0.92	−5.7
B−H_{term}	exp	1.18	1.18	1.40(4)	−12.2(16)
	B3/exp	1.18	1.18	1.25	−7.4
	B3/opt	1.19	1.19	1.24	−7.5
	HF/opt	1.18	1.18	1.23	−4.1
	MP2/opt	1.19	1.19	1.22	−4.0
	B3+/opt	1.18	1.18	1.27	−9.5
long B−H_{bridge}	exp	1.42	1.47	0.70(5)	−1(1)
	B3/exp	1.42	1.51	0.70	0.3
	B3/opt	1.41	1.52	0.70	0.17
	HF/opt	1.43	1.53	0.63	3.6
	MP2/opt	1.42	1.55	0.67	3.0
	B3+/opt	1.41	1.51	0.72	−0.39
short B−H_{bridge}	exp	1.26	1.27	1.06(2)	−7.2(2)
	B3/exp	1.26	1.26	0.94	1.9
	B3/opt	1.26	1.27	0.93	1.8
	HF/opt	1.25	1.26	0.96	5.5
	MP2/opt	1.26	1.27	0.91	5.3
	B3+/opt	1.25	1.26	0.96	0.06
ring critical points	exp			0.61(2)	0.6(1)
	B3/exp			0.64	−0.9
	B3/opt			0.63	−0.88
	HF/opt			0.59	−1.20
	MP2/opt			0.63	−1.60
	B3+/opt			0.65	−1.20

[a] "distance" gives the length of the direct interatomic vector, while "path" gives the length of the bond path. B−H bonds are fixed on theoretical distances.[17] Theoretical values of ρ_{BCP} and $\nabla^2\rho_{BCP}$ were obtained from various theoretical calculations[22] (*Gaussian*[23]).

2e-3c systems occur in dihydrogen complexes or agostic interactions and, as described herein, hydride bridges. Depending on the kind of interaction, the common picture of ring structures should be abandoned.[26] As in tetraborane, hydride bridges are often asymmetric. This asymmetry is shown not only in the structure but also in the topological properties. The values of the electron density at the BCPs (Table 1) show that the shorter B−H_{bridge} bonds are higher populated than the longer bonds, with a fair agreement between experiment and theory. Generally, covalent and ionic interactions can be distinguished by the sign of the Laplacian at the BCP, in that a negative/positive Laplacian should indicate a covalent/closed-shell interaction. The experimental and theoretical Laplacians of the B−H_{term} bonds are all negative, with considerably negative experimental values compared to theory. The findings for the hydride bridges are significantly different. From the experiment, highly negative values are derived for the short B−H_{bridge}, whereas the long ones have small negative values. The theoretical Laplacians are in part positive and negative and differ strongly between the different types of calculations. Moreover, nothing can be concluded between the shorter and longer B−H_{bridge} bonds. This is in line with theoretical calculations by Bader et al., who reported Laplacians for hydride bridges in boranes on "both sides of zero".[7] Thus, no definite conclusion can be drawn only from the values of the Laplacians at the BCPs if $\nabla^2\rho_{BCP}$ is close to zero.

However, the two-dimensional plot of the experimental Laplacian distribution (Figure 2, middle) allows further insight

(16) Crystal Impact. *DIAMOND*, version 3.1; Crystal Impact GbR: Bonn, Germany, 2006.

(17) (a) Bühl, M.; Schleyer, P. v. R. *J. Am. Chem. Soc.* **1992**, *114*, 477–491. (b) Brain, P. T.; Morrison, C. A.; Parsons, S.; Rankin, D. W. H. *J. Chem. Soc., Dalton Trans.* **1996**, 4589–4596.

(18) For details, see the Supporting Information.

(19) Hansen, N. K.; Coppens, P. *Acta Crystallogr.* **1978**, *A34*, 909.

(20) Koritsánszky, T.; et al. *XD, A Computer Program Package for Multipole Refinement and Analysis of Electron Densities from Diffraction Data*; Freie Universität Berlin: Berlin, Germany, 2004.

(21) (a) Bader, R. F. W. *Atoms in Molecules*, 2nd ed.; Clarendon Press: Oxford, U.K., 1995. (b) Bader, R. F. W. In *The Encyclopedia of Computational Chemistry*; Schleyer, P. v. R., et al., Eds.; Wiley: Chichester, U.K., 1998. (c) Bader, R. F. W.; Popelier, P. L. A.; Keith, T. A. *Angew. Chem.* **1994**, *106*, 647–659. (d) Bader, R. F. W.; Popelier, P. L. A.; Keith, T. A. *Angew. Chem., Int. Ed. Engl.* **1994**, *33*, 620–631.

(22) Theoretical topological properties were obtained from the following ab initio calculations:[23] HF/6-311G** (HF/opt), MP2/6-311G** (MP2/opt), B3LYP/6-311G** (B3/opt), and B3LYP/6-311G^{++}G(3df,3pd) (B3+/opt) geometry optimizations and B3LYP/6-311G** (B3/exp) at experimental geometry.

(23) Frisch, M. J.; et al. *Gaussian 98*, revision A.7; Gaussian Inc.: Pittsburgh, PA, 1998.

(24) Haaland, A.; Shorokhov, D. J.; Tverdova, N. V. *Chem.—Eur. J.* **2004**, *10*, 4416–4421.

(25) Farrugia, L. A.; Evans, C.; Tegel, J. *J. Phys. Chem. A* **2006**, *110*, 7952–7961.

(26) Macchi, P.; Sironi, A. In *The Quantum Theory of Atoms in Molecules*; Matta, C. F., Boyd, R. J., Eds.; Wiley-VCH: Weinheim, Germany, 2007; p 356.

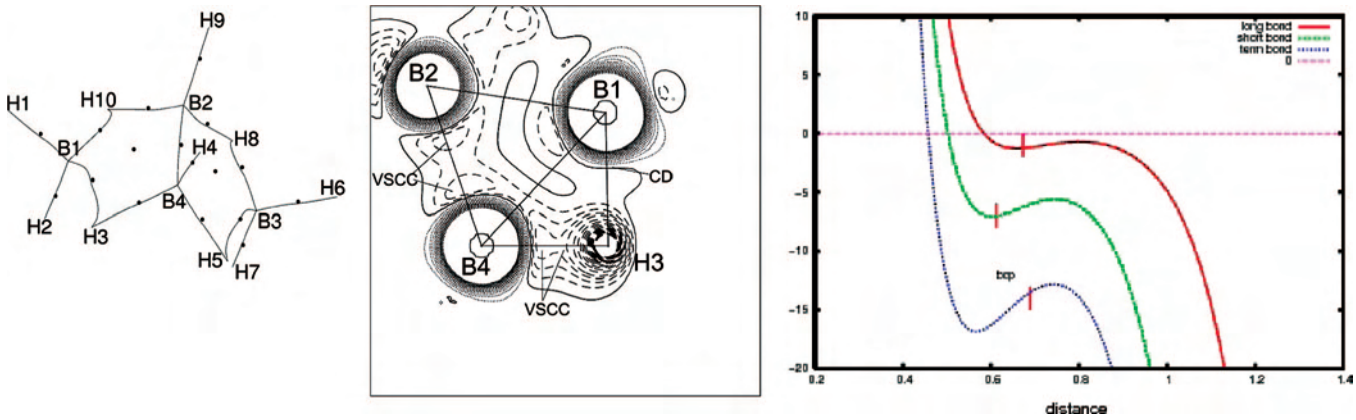

Figure 2. Left: Curvature of the bond paths in tetraborane(10). Black dots: BCP and RCPs, respectively. Middle: Two-dimensional plot of the Laplacian distribution from the experimental density of a 2e-3c bond in tetraborane (B1−H3−B4). Increments: 2.5 e/Å^5. Right: Experimental Laplacian along the bond path (B, left; H, right) of three B−H bonds in tetraborane. BCPs are drawn as a short red line in each curve.

into such ambiguous situations. If second-row atoms are covalently bonded, the *valence shell charge concentrations* (VSCC, minima of $\nabla^2\rho$) along the bond path overlap partially. In the bond center, $\nabla^2\rho$ is smaller than zero and a saddle-shaped region is formed that is typical for an *open-shell* interaction.[26] This can be seen clearly at the covalent B2−B4 bond. When a covalent bond is significantly polarized, the BCP is shifted toward the VSCC of the less electronegative atom; eventually, both VSCCs merge in the region of the more electronegative atom. This can be seen in the case of the shorter and higher populated B−H_{bridge} bond (B4−H3; Figure 2). The VSCC of B4 is no longer separated but shifted in the direction of the electronegative H3. In contrast to this, the longer B1−H3 bond shows neither a VSCC nor a charge accumulation along the bond path. The topological situation for the B−H bonds in question is further illustrated by the plots of the Laplacians along the bond paths as shown in Figure 2 (right), where also for comparison the terminal 2e-2c B−H_{term} bond is shown. On the latter one, the saddle-shaped region is clearly seen. A pronounced decrease of this feature is visible when going via the short 2e-3c B−H_{bridge} bond to the longer one. Thus, a decrease of covalency of the B−H bonds can be observed on going from the terminal to the bridging bonds.

The electrostatic potential (ESP; Figure 3) of the title compound was calculated from the experimental charge density using the method of Su and Coppens.[27] In tetraborane(10), the B atoms are positively polarized. Toroidal regions of negative potential are seen around the H atoms, which could be expected because of the higher electronegativity of the H atoms compared to that of the B atoms.

This is supported by the atomic charges obtained experimentally from the Bader formalism (see Table S1 of the Supporting Information). The experimental hydrogen charges

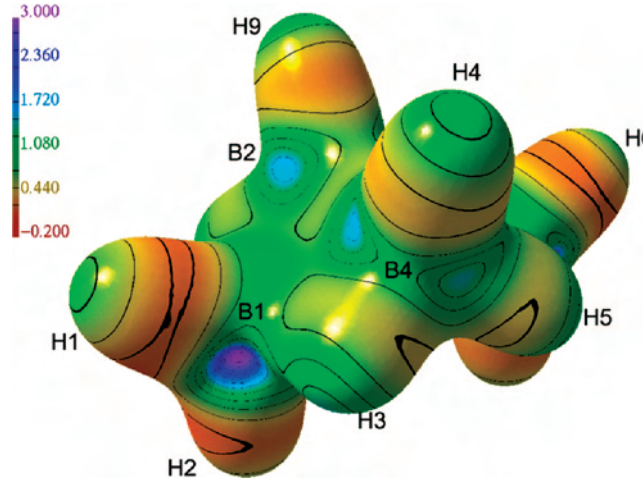

Figure 3. Plot of the ESP, which is mapped on the electron density surface at 0.5 e/Å^3 by a color gradient: red, negative values in ESP; blue, positive ESP values. Mol*Iso* drawing.[28]

average to –0.3(1) e, while the corresponding average of the boron charges is 0.79(5) e,[18] resulting in an average charge separation of 1.09 e between B and H. Formally, the B_4H_{10} molecule can be separated into one $B_2H_6^{2-}$ fragment, which bonds to two BH_2^+ fragments. Addition of the Bader charges for these fragments results in +0.22 e and –0.41 e from the experiment and stronger differences from theory depending on the type of calculation (+0.52 e to +0.68 e and −1.02 e to –1.36 e, respectively; Table S2 of the Supporting Information).

Acknowledgment. This work was supported by the DFG, SPP 1178, and Grants Le 423/13-2 and Lu 222/30-2.

Supporting Information Available: Synthesis and crystal growth, X-ray crystallographic data in CIF format and tables of atomic properties (Table S1) and sum of Q_{001} charges (Table S2). This material is available free of charge via the Internet at http://pubs.acs.org.

IC701924R

(27) Su, Z. W.; Coppens, P. *Acta Crystallogr., Sect. A* **1992**, *48*, 188.
(28) Hübschle, C. B.; Luger, P. *J. Appl. Crystallogr.* **2006**, *39*, 901.
(29) Sheldrick, G. M. *SHELXS97*: University of Göttingen; Göttingen, Germany, 1997.